Dynamic Behaviours of Non-Uniform Rayleigh Beam under Variable-Magnitude Accelerating Masses and Resting on Non-Uniform Bi-parametric Foundation with General Boundary Conditions

Abstract

This paper investigates the dynamic behaviours of non-uniform Rayleigh beam under variable-magnitude accelerating masses and resting on non-uniform bi-parametric foundation with general boundary conditions. The problem is governed by a fourth-order partial differential equation, generalised Galerkin's method use to reduces the fourth-order partial differential equation to sequence second-order ordinary differential equations. Two cases are examined: moving force (neglecting inertia term) and moving mass (considering inertia). In order to solve the moving force problem, the transverse displacement response is obtained by variation of parameters. In order to solve the moving mass problem, the Runge-Kutta of fourth order is used to obtain the approximate solution because the commonly used Struble asymptotic method was unable to simplify the coupled second order ordinary differential equation due to the variability of the load magnitude. Analytical and numerical solutions (Runge-Kutta) are compared for validation of accuracy of the Runge-kutta scheme and found compared favourably. The results are presented in plotted curves, illustrating the effects of shear modulus, rotatory inertia correction factor results show increased shear moduli and rotatory inertia decrease response amplitudes, and critical speed for moving mass is lower than for moving force, leading to earlier resonance. Resonance conditions for the dynamical system are also established.

Keywords: Non-uniform Rayleigh beam, bi-parametric foundation, moving force, moving mass, Galerkin's Method, Runge-Kutta.

1 Introduction

This paper is sequel to an earlier work by [1] which investigated the dynamic behaviour of simply supported non-uniform Rayleigh beams under variable-magnitude accelerating masses on non-uniform bi-parametric foundations. Specifically, this study generalizes the theoretical framework presented in [1] to provide a more comprehensive understanding of the dynamic response of non-uniform Rayleigh beams under variable-magnitude accelerating masses and resting on non-uniform bi-parametric foundations. Beam dynamics is a vital aspect of structural engineering and mechanical systems, particularly in complex loading and foundation scenarios. The Rayleigh beam theory, which accounts for rotating inertia and shear deformation, has become a widely accepted model for understanding beam behaviour. Research into the dynamic responses of structural members on elastic foundations subjected to moving loads is crucial, with applications in enhancing our understanding of dynamic characteristics in various fields, including transportation infrastructure, aerospace and mechanical engineering. The works of several researchers, including [2], [3], [4], [5] and [6], have made significant contributions to this field. The dynamic response of beams subjected to accelerating loads is a multifaceted challenge traversing various engineering disciplines. Specifically, it is pivotal in high-speed transportation systems, where rail vibrations impact passenger safety and comfort. In aerospace engineering, understanding beam dynamics under accelerating loads ensures structural integrity and stability of aircraft wings, helicopter rotor blades, and spacecraft components. Civil engineers must consider dynamic responses when designing bridges and buildings to withstand seismic activity, wind loads, and vehicular traffic. Moreover, mechanical engineers rely on accurate beam analysis to optimize gearbox and transmission systems, rotating machinery, and machine tools. Industrial machinery, including conveyor belts and vibrating screens, also requires precise dynamic modeling to enhance performance and reliability. In most of the work of dynamic response of non-uniform beam available in literature, when the beam is under variable-magnitude accelerating loads is a neglected in there area of research, as evidenced by the works of [2], [6], [7], [8], [4] and [9]. Model complexity and challenges in parameter estimation have limited the investigation of beams subjected to variable-magnitude accelerating loads.

[10] investigated dynamic behaviour under moving distributed masses of non-uniform Rayleigh beam with general boundary conditions. Their study provided valuable insights into the effects of foundation moduli and rotatory inertia correction factor on the response amplitudes of the beam. However, their work focused on loads with constant magnitude, leaving a knowledge gap regarding the dynamic response of such beams to loads with variable magnitude. This study aims to address this gap by exploring the flexural vibration of a non-uniform Rayleigh beam subjected to variable-magnitude accelerating masses. In real-world applications, non-uniform beams are frequently subjected to variable-magnitude accelerating loads, significantly impacting their dynamic behaviuor. Examples include high-speed transportation systems, where railways and maglev trains exert variable-magnitude accelerating loads on bridge structures and rail tracks; aerospace engineering, where aircraft wings experience accelerating loads during takeoff, landing and maneuvering; industrial machinery, such as conveyor belts and vibrating screens; construction, where cranes and elevators subject building frames to accelerating loads; and vibration-based energy harvesting systems. Despite their prevalence, existing research has primarily focused on simplified loading conditions, neglecting the complexities of variable-magnitude accelerating loads. Accurate modeling is crucial for ensuring structural integrity, optimizing beam design and reducing material costs. However, mathematical model complexity and parameter estimation challenges have hindered comprehensive investigation, creating a significant knowledge gap that

necessitates further research. This study pays special attention to the situation in which the beam rests on a bi-parametric basis and is subjected to variable-magnitude accelerating load.

2 Mathematical Model

Consider a non-uniform Rayleigh beam of length L, resting on a non-uniform bi-parametric foundation, and subjected to accelerating masses and a traveling distributed load with significant inertia, neglecting damping. The beam's vibration is governed by the fourth-order partial differential equation given in by [11] as follows

$$\frac{\partial^2}{\partial x^2}\left[EJ(x)\frac{\partial^2 q^*(x,t)}{\partial x^2}\right]-N\frac{\partial^2 q^*(x,t)}{\partial x^2}+\mu^*(x)\frac{\partial^2 q^*(x,t)}{\partial t^2}-\mu^*(x)R_0\frac{\partial^4 q^*(x,t)}{\partial x^2\partial t^2}+F_k(x,t)q^*(x,t)) = P^*(x,t) \tag{1}$$

$EJ(x)$ is the variable flexural rigidity of the structure, t is the time co-ordinate, x is the spatial co-ordinate, $q^*(x,t)$ is the transverse displacement, $\mu^*(x)$ is the variable mass per unit length of non-uniform beam, N is the axial force, R_0 is the rotatory inertia factor, $F_k(x,t)$ is the variable foundation reaction, $F^*(x,t)$ is the travelling load.

The non-uniform bi-parametric foundation in this system is modeled to be of the form:

$$F_k(x,t)q^*(x,t) = S(x)q^*(x,t) - G'(x)\frac{\partial}{\partial x}q^*(x,t) - G(x)\frac{\partial^2}{\partial x^2}q^*(x,t) \tag{2}$$

where $S(x)$ is the variable foundation stiffness and $G(x)$ is the variable shear modulus.

Considering the influence of moving loads on beam response, the load $F^*(x,t))$ takes the form

$$F^*(x,t) = Q_f(x,t)\left[1 - \frac{d^2}{dt^2}\left[\frac{q^*(x,t)}{g}\right]\right] \tag{3}$$

where the continous moving force $Q_f(x,t)$ acting on the beam model is given by

$$Q_f(x,t) = Mg\cos\omega t H(x - P^*(t)) \tag{4}$$

$P^*(t)$ is the distance traversed by the load at any time instant t is given by:

$$P^*(t) = x_o + ct + \frac{1}{2}at^2 \tag{5}$$

where x_0 denote the point of application of the force $Q_f(x,t)$ at any given instance. $t = 0$, c is the initial velocity, a is the constant acceleration of motion.

Since the load is taken to be the mass M and time t taken to be limited to the interval of the time

$$0 \leq P^*(t) \leq L \tag{6}$$

and the $H(x - P^*(t))$ is the heaviside function which is defined as

$$H(x - P^*(t)) = \begin{cases} 0, & x < P^*(t); \\ 1, & x \geq P^*(t). \end{cases} \tag{7}$$

with the properties

i

$$\frac{d}{dx}\big(H(x-P^*(t))\big)=\delta(x-P^*(t)) \tag{8}$$

ii

$$f(x)H(x-P^*(t))=\begin{cases}0, & x<P^*(t);\\ f(x), & x>P^*(t).\end{cases} \tag{9}$$

where $\delta(x-P^*(t))$ represents the Dirac delta function defined as follows:

i

$$\delta(x-P^*(t))=\begin{cases}0, & x\neq P^*(t);\\ \infty, & x=P^*(t).\end{cases} \tag{10}$$

ii

$$\delta(x)=\begin{cases}0, & x\neq 0;\\ \infty, & x=0.\end{cases} \tag{11}$$

with the properties

i

$$\delta(x)=\delta(-x) \tag{12}$$

ii

$$\int_a^b \delta(x-k)f(x)dx=\begin{cases}0, & k<a<b;\\ f(k), & a<k<b;\\ 0, & a<b<k\\ .\end{cases} \tag{13}$$

g is the acceleration due to gravity and $\frac{d^2}{dt^2}$ is a convective acceleration define by [11].

$$\frac{d^2}{dt^2}=\frac{\partial^2}{\partial t^2}+2\frac{d}{dt}P^*(t)\frac{\partial^2}{\partial x\partial t}+\left(\frac{dP^*(t)}{dt}\right)\frac{\partial^2}{\partial x^2}+\frac{d^2}{dt^2}\left(P^*(t)\right)\frac{\partial}{\partial x} \tag{14}$$

As an example in the problem [12], $S(x)$ and $G(x)$ take the form

$$S(x)=S_0(4x-3x^2+x^3) \text{ and } G(x)=G_0(12-13x+6x^2+x^3) \tag{15}$$

S_0 is the foundation constant and G_0 is a constant shear modulus.

Also adopting example [13], $J(x)$ and $\mu^*(x)$ are taken to be of the form

$$J(x)=J_0(1+\sin\frac{\pi x}{L})^3 \text{ and } \mu^*(x)=\mu_o(1+\sin\frac{\pi x}{L}) \tag{16}$$

substituting equation (2), (3), (4), (14), (15) and (16) into equation (1) after some simplifications and rearrangements one obtains

$$
\frac{EJ_0}{4}\left[\frac{\partial^2}{\partial x^2}\left(10+15\sin\frac{\pi x}{L}-6\cos\frac{2\pi x}{L}-\sin\frac{3\pi x}{L}\right)\frac{\partial^2 q^*(x,t)}{\partial x^2}\right]-N\frac{\partial^2 q^*(x,t))}{\partial x^2}+\mu_0\left(1+\sin\frac{\pi x}{L}\right)\frac{\partial^2 q^*(x,t)}{\partial t^2}
-\mu_0\left(1+\sin\frac{\pi x}{L}\right)R_0\frac{\partial^4 q^*(x,t)}{\partial x^2\partial t^2}+S_0\left(4x-3x^2+x^3\right)q^*(x,t))-G_0\left(-13+12x+3x^2\right)\frac{\partial}{\partial x}q^*(x,t)
-G_0\left(12-13x+6x^2+x^3\right)\frac{\partial^2}{\partial x^2}q^*(x,t)+M\cos\omega t H\left[x-\left(x_o+ct+\frac{1}{2}at^2\right)\right]\left[\frac{\partial^2}{\partial t^2}+2(c+at)\frac{\partial^2}{\partial x\partial t}+
(c+at)^2\frac{\partial^2}{\partial x^2}+a\frac{\partial}{\partial x}\right]q^*(x,t)=Mg\cos\omega t H\left[x-\left(x_o+ct+\frac{1}{2}at^2\right)\right]
\tag{17}
$$

It is assumed that the initial conditions are

$$
q^*(x,0)=0=q^*_{tt}(x,0) \tag{18}
$$

3 Solution technique

Equation (17) presents a fourth-order partial differential equation with variable coefficients, governing the dynamics of the non-uniform Rayleigh beam subjected to traveling variable magnitude distributed loads. Due to its complexity, an exact solution is unattainable. To address this, an approximate analytical solution is sought using the Generalized Galerkin Method (GGM), as described in [11]. This technique involves simplifying and reducing Equation (17) to a set of second-order ordinary differential equations, known as Galerkin equations. In order to use GGM, it is assumed that the solution to Equation (17) take the form:

$$
q^*_j(x,t)=\sum_{j=1}^{\infty}Q_j(t)Z_j(x) \tag{19}
$$

where $Z_j(x)$ is chosen such that the pertinent boundary conditions are satisfied. Substituting (17) into (19) and after some simplifications and arrangements, one obtains

$$
\sum_{i=1}^{N}\Bigg[\Bigg(\left(Z_j(x)+\sin\frac{\pi x}{L}(Z_j(x))-R_0(Z_j''(x)+\sin\frac{\pi x}{L}Z_j''(x))\right)\ddot{Q}_j(t)+\Bigg(\frac{EJ_0}{4\mu_0}\Bigg(10Z_j^{iv}(x)+15\sin\frac{\pi x}{L}Z_j^{iv}(x)
-6\cos\frac{2\pi x}{L}Z_j^{iv}(x)-\sin\frac{3\pi x}{L}Z_j^{iv}(x)-\frac{30\pi}{L}\cos\frac{\pi x}{L}Z_j'''(x)+\frac{24\pi}{L}\sin\frac{2\pi x}{L}Z_j'''(x)-\frac{6\pi}{L}\cos\frac{3\pi x}{L}Z_j'''(x)
-\frac{15\pi^2}{L^2}\sin\frac{\pi x}{L}Z_j''(x)+\frac{24\pi^2}{L^2}\cos\frac{2\pi x}{L}Z_j''(x)+\frac{9\pi^2}{L^2}\sin\frac{3\pi x}{L}Z_j''(x)\Bigg)-\frac{N_0}{\mu_0}Z_j''(x)
+\frac{S_0}{\mu_0}\left(4xZ_j(x)-3x^2Z_j(x)+x^3Z_j(x)\right)-\frac{G_0}{\mu_0}\Bigg(-13Z_j'(x)+12xZ_j'(x)+3x^2Z_j'(x)+12Z_j''
(x)-13xZ_j''(x)-6x^2Z_j''(x)+x^3Z_j''(x)\Bigg)\Bigg]Q_j(t)+\sum_{i=1}^{N}\frac{M\cos\omega t}{\mu_0}\Bigg(H\left[x-\left(x_o+ct+\frac{1}{2}at^2\right)\right]Z_j(x)\ddot{Q}_j(t)
+2(c+at)H\left[x-\left(x_o+ct+\frac{1}{2}at^2\right)\right]Z_j'(x)\dot{Q}_j(t)+(c+at)^2H\left[x-\left(x_o+ct+\frac{1}{2}at^2\right)\right]Z_j''(x)Q_j(t)+
aH\left[x-\left(x_o+ct+\frac{1}{2}at^2\right)\right]Z_j'(x)Q_j(t)\Bigg)-\frac{Mg\cos\omega t}{\mu_0}H\left[x-\left(x_o+ct+\frac{1}{2}at^2\right)\right]=0
\tag{20}
$$

In order to determine $Q_j(t)$, it is required that the expression on the right hand side of equation (20) be orthogonal to function $Z_k(x)$.

Thus, equation (20) becomes

$$
\begin{aligned}
&\Bigg\{ \int_0^L \sum_{i=1}^{N} \Bigg\{ \Bigg((Z_j(x)Z_k(x) + \sin\frac{\pi x}{L}(Z_j(x)Z_k(x)) - R_0(Z_j''(x)Z_k(x) + \sin\frac{\pi x}{L} Z_j''(x)Z_k(x)) \Bigg) \ddot{Q}_j(t) + \\
&\Bigg\{ \frac{EI_0}{4\mu_0} \Bigg(10Z_j^{iv}(x)Z_k(x) + 15\sin\frac{\pi x}{L} Z_j^{iv}(x)Z_k(x) - 6\cos\frac{2\pi x}{L} Z_j^{iv}(x)Z_k(x) - \sin\frac{3\pi x}{L} Z_j^{iv}(x)Z_k(x) \\
&- \frac{30\pi}{L}\cos\frac{\pi x}{L} Z_j'''(x)Z_k(x) + \frac{24\pi}{L}\sin\frac{2\pi x}{L} Z_j'''(x)Z_k(x) - \frac{6\pi}{L}\cos\frac{3\pi x}{L} Z_j'''(x)Z_k(x) - \frac{15\pi^2}{L^2}\sin\frac{\pi x}{L} Z_j''(x)Z_k(x) \\
&+ \frac{24\pi^2}{L^2}\cos\frac{2\pi x}{L} Z_j''(x)Z_k(x) + \frac{9\pi^2}{L^2}\sin\frac{3\pi x}{L} Z_j''(x)Z_k(x) \Bigg) - \frac{N_0}{\mu_0} U_j''(x)U_k(x) + \frac{S_0}{\mu_0}\Bigg(4xZ_j(x)Z_k(x) - \\
&3x^2 Z_j(x)Z_k(x) + x^3 Z_j(x)Z_k(x) \Bigg) - \frac{G_0}{\mu_0}\Bigg(-13U_j'(x)Z_k(x) + 12xZ_j'(x)Z_k(x) + 3x^2 Z_j'(x)Z_k(x) \\
&+ 12Z_j''(x)Z_k(x) - 13xZ_j''(x)Z_k(x) - 6x^2 Z_j''(x)Z_k(x) + x^3 Z_j''(x)Z_k(x) \Bigg) \Bigg\} Q_j(t) \\
&+ \sum_{i=1}^{N} \frac{M\cos\omega t}{\mu_0} \Bigg(H(x-f(t))Z_j(x)Z_k(x)\ddot{Q}_j(t) + 2(c+at)H(x-f(t))Z_j'(x)Z_k(x)\dot{Q}_j(t) \\
&+ (c+at)^2 H(x-f(t))Z_j''(x)Z_k(x)Q_j(t) + aH(x-f(t))Z_j'(x)Z_k(x)Q_j(t) \Bigg) \\
&- \frac{Mg\cos\omega t}{\mu_0} H(x-f(t))Z_k(x) \Bigg\} dx = 0
\end{aligned}
\tag{21}
$$

After simplification and arrangement of equation (21) one gets

$$
\begin{aligned}
&\sum_{j=0}^{N} \Bigg\{ \Bigg((A_0(j,k) + A_1(j,k)) - R_0(A_2(j,k) + A_3(j,k)) \Bigg) \ddot{Q}_j(t) + \Bigg(W_A \Bigg(10A_4(j,k) - 15A_5(j,k) \\
&- 6A_6(j,k) - A_7(j,k) + \frac{30\pi}{L}A_8(j,k) + 24\frac{\pi}{L}A_9(j,k) - 6\frac{\pi}{L}A_{10}(j,k) - 15\frac{\pi^2}{L}A_{11}(j,k) \\
&+ 24\frac{\pi^2}{L}A_{12}(j,k) + 3\frac{\pi^2}{L}A_{13}(j,k) \Bigg) - W_B A_{14}(j,k) - W_C\Bigg(4A_{15}(j,k) - 3B_{16}(j,k) + A_{17}(j,k) \Bigg) \\
&- W_D\Bigg(-13A_{18}(j,k) + 12A_{19}(j,k) - 3A_{20}(j,k) + 12A_{21}(j,k) - 13A_{22}(j,k) - 6A_{23}(j,k) \\
&- A_{24}(j,k) \Bigg) \Bigg) Q_j(t) + \frac{M\cos\omega t}{\mu_0} \Bigg(A_{25}(j,k)\ddot{Q}_j(t) + 2(c+at)B_{26}(j,k)\dot{Q}_j(t) \\
&+ (c+at)A_{27}(j,k)Q_j(t) + aA_{28}(j,k)Q_j(t) \Bigg) \Bigg\} = \frac{Mg\cos\omega t}{\mu_0} A_{29}(t)
\end{aligned}
\tag{22}
$$

where

$$
W_A = \frac{4I_0}{\mu_0}, \quad W_B = \frac{N_0}{\mu_0}, \quad W_C = \frac{S_0}{\mu_0} \quad W_D = \frac{G_0}{\mu_0}
$$

$$
A_0(j,k) = \int_0^L Z_j(x)Z_k(x)dx
$$

$$
A_1(j,k) = \int_0^L \sin\frac{\pi x}{L} Z_j(x)Z_k(x)dx
$$

$$
A_2(j,k) = \int_0^L Z_j''(x)Z_k(x)
$$

$$A_3(j,k) = \int_0^L \sin\frac{\pi x}{L} Z_j''(x) Z_k(x) dx$$

$$A_4(j,k) = \int_0^L Z_j^{iv}(x) Z_k(x) dx$$

$$A_5(j,k) = \int_0^L \sin\frac{\pi x}{L} Z_j^{iv}(x) Z_k(x) dx$$

$$A_6(j,k) = \int_0^L \cos\frac{2\pi x}{L} Z_j^{iv}(x) Z_k(x) dx$$

$$A_7(j,k) = \int_0^L \sin\frac{3\pi x}{L} Z_j^{iv}(x) Z_k(x) dx$$

$$A_8(j,k) = \int_0^L \cos\frac{\pi x}{L} Z_j'''(x) Z_k(x) dx$$

$$A_9(m,k) = \int_0^L \sin 2\frac{\pi x}{L} Z_j'''(x) Z_k(x) dx$$

$$A_{10}(j,k) = \int_0^L \cos 3\frac{\pi x}{L} Z_j'''(x) Z_k(x) dx$$

$$A_{11}(j,k) = \int_0^L \sin\frac{\pi x}{L} Z_j''(x) Z_k(x) dx$$

$$A_{12}(j,k) = \int_0^L \cos 2\frac{\pi x}{L} Z_j''(x) Z_k(x) dx$$

$$A_{13}(j,k) = \int_0^L \sin 3\frac{\pi x}{L} Z_j''(x) Z_k(x) dx$$

$$A_{14}(j,k) = \int_0^L Z_j(x) Z_k(x) dx$$

$$A_{15}(j,k) = \int_0^L x Z_j(x) Z_k(x) dx$$

$$A_{16}(j,k) = \int_0^L x^2 Z_j(x) Z_k(x) dx$$

$$A_{17}(j,k) = \int_0^L x^3 Z_j(x) Z_k(x) dx$$

$$A_{18}(j,k) = \int_0^L Z_j'(x) Z_k(x) dx$$

$$A_{19}(j,k) = \int_0^L x Z_j'(x) Z_k(x) dx$$

$$A_{20}(j,k) = \int_0^L x^2 Z_j'(x) U_k(x) dx$$

$$A_{21}(j,k) = A_2(m,k)$$

$$A_{22}(j,k) = \int_0^L x Z_j''(x) Z_k(x) dx$$

$$A_{23}(j,k) = \int_0^L x^2 Z_j''(x) Z_k(x) dx$$

$$A_{24}(j,k) = \int_0^L x^2 Z_j''(x) Z_k(x) dx$$

$$A_{25}(j,k) = \int_0^L H\left[x - \left(x_o + ct + \frac{1}{2}at^2\right)\right] Z_j(x) Z_k(x) dx$$

$$A_{26}(j,k) = \int_0^L H\left[x - \left(x_o + ct + \frac{1}{2}at^2\right)\right] Z_j'(x) Z_k(x) dx$$
$$A_{27}(j,k) = \int_0^L H\left[x - \left(x_o + ct + \frac{1}{2}at^2\right)\right] Z_j''(x) Z_k(x) dx$$
$$A_{28}(j,k) = A_{26}(j,k)$$
$$A_{29}(j,k) = \int_0^L H\left[x - \left(x_o + ct + \frac{1}{2}at^2\right)\right] Z_k(x) dx \tag{23}$$

In order to solve this equation, Using the Fourier series representation of the Heaviside unit step function, namely,

$$H(x - p^*(t)) = \frac{1}{4} + \frac{1}{\pi}\sum_0^\infty \frac{\sin(2n+1)\pi(x - p^*(t))}{(2n+1)}, \qquad 0 < x < L \tag{24}$$

and an appropriate selection of beam function $Z_j(x)$:

$$Z_j(x) = \sin\frac{a_j x}{L} + A_j \cos\frac{a_i x}{L} + B_j \sinh\frac{a_j x}{L} + C_j \cosh\frac{a_j x}{L} \tag{25}$$

so that

$$Z_k(x) = \sin\frac{a_k x}{L} + A_k \cos\frac{a_k x}{L} + B_k \sinh\frac{a_k x}{L} + C_k \cosh\frac{a_k x}{L} \tag{26}$$

The unknown constants A_j, B_j, C_j, A_k, B_k, C_k and the natural frequencies a_j, a_k are obtained by applying classical boundary conditions. Substituting equation (24), (25) and (26) into (22) after some simplification and rearrangement, one obtains.

$$D_0(j,k)\ddot{Q}_j(t) + D_1(j,k)Z_m(t) + \epsilon_0 \cos\omega t\Bigg\{L\left(\frac{1}{4}B_1(j,k) + \frac{1}{\pi}\sum_0^\infty \frac{\cos(2n+1)\pi(x_0 + ct + \frac{1}{2}at^2)}{(2n+1)} B_{1a}(n,j,k) - \right.$$
$$\left.\frac{1}{\pi}\sum_0^\infty \frac{\sin(2n+1)\pi(x_0 + ct + \frac{1}{2}at^2)}{(2n+1)} B_{1b}(n,j,k)\right)\ddot{Q}_j(t) + 2L(c+at)\left(\frac{1}{4}Q_2(j,k) + \right.$$
$$\left.\frac{1}{\pi}\sum_0^\infty \frac{\cos(2n+1)\pi(x_0 + ct + \frac{1}{2}at^2)}{(2n+1)} B_{2a}(n,j,k) - \frac{1}{\pi}\sum_0^\infty \frac{\sin(2n+1)\pi(x_0 + ct + \frac{1}{2}at^2)}{(2n+1)} B_{2b}(n,j,k)\right)\dot{Q}_j(t)$$
$$+\Bigg(L(c+at)^2\left(\frac{1}{4}B_3(j,k) + \frac{1}{\pi}\sum_0^\infty \frac{\cos(2n+1)\pi(x_0 + ct + \frac{1}{2}at^2)}{(2n+1)} B_{3a}(n,j,k)\right.$$
$$\left.-\frac{1}{\pi}\sum_0^\infty \frac{\sin(2n+1)\pi(x_0 + ct + \frac{1}{2}at^2)}{(2n+1)} B_{3b}(n,j,k)\right) + La\left(\frac{1}{4}B_2(j,k)\right.$$
$$\left.\left.+\frac{1}{\pi}\sum_0^\infty \frac{\cos(2n+1)\pi(x_0 + ct + \frac{1}{2}at^2)}{(2n+1)} B_{2a}(n,j,k) - \frac{1}{\pi}\sum_0^\infty \frac{\sin(2n+1)\pi(x_0 + ct + \frac{1}{2}at^2)}{(2n+1)} B_{2b}(n,j,k)\right)\Bigg)Q_j(t)\Bigg\}$$
$$= \frac{LMg\cos\omega t}{a_k\mu_0}\Bigg(\theta_{JC} + \cos\frac{a_k}{L}(x_0 + ct + \frac{1}{2}at^2) - A_k + \sin\frac{a_k}{L}(x_0 + ct + \frac{1}{2}at^2) - B_k + \cosh\frac{a_k}{L}(x_0 + ct + \frac{1}{2}at^2)$$
$$- C_k + \sinh\frac{a_k}{L}(x_0 + ct + \frac{1}{2}at^2)\Bigg) \tag{27}$$

where

$$\theta_{JC} = -\cos a_k + A_k \sin a_k + B_k \cosh a_k + C_k \sinh a_k$$

$$B_1(j,k) = A_0(j,k)$$
$$B_{1A}(n,j,k) = \int_0^L sin(2n+1)\pi x Z_j(x) Z_k(x) dx$$
$$B_{1B}(n,j,k) = \int_0^L cos(2n+1)\pi x Z_j(x) Z_k(x) dx$$
$$B_2(j,k) = A_{18}(m,k)$$
$$B_{2A}(n,j,k) = \int_0^L sin(2n+1)\pi x Z_j'(x) Z_k(x) dx$$
$$B_{2B}(n,j,k) = \int_0^L cos(2n+1)\pi x Z_j'(x) Z_k(x) dx$$
$$B_3(j,k) = A_2(m,k)$$
$$B_{3A}(n,j,k) = \int_0^L sin(2n+1)\pi x Z_j''(x) Z_k(x) dx$$
$$B_{3B}(n,j,k) = \int_0^L cos(2n+1)\pi x Z_j''(x) Z_k(x) dx$$
$$\epsilon_0 = \frac{M}{\mu_0 L} \tag{28}$$

ϵ_0 is the inertia term.

Equation (27) governs the dynamic behaviour of non-uniform Rayleigh beams under variable-magnitude accelerating masses and resting on non-uniform bi-parametric foundations. Two special cases are now discussed.

4 Closed Form Solution

4.1 Non-uniform Rayleigh Beam Traversed by Moving Force

By assuming negligible inertia (ϵ_0) in equation (27), an approximate solution for the dynamic problem is obtained as

$$D_0(m,k)\ddot{Q}_j(t) + D_1(j,k)Q_j(t) = \frac{LMg\cos\omega t}{a_k \mu_0}\Big(\theta_{JC} + \cos\frac{a_k}{L}(x_0 + ct + \frac{1}{2}at^2) - A_k + \sin\frac{a_k}{L}(x_0 + ct + \frac{1}{2}at^2)$$
$$- B_k + \cosh\frac{a_k}{L}(x_0 + ct + \frac{1}{2}at^2) - C_k + \sinh\frac{a_k}{L}(x_0 + ct + \frac{1}{2}at^2)\Big) \tag{29}$$

Rearrangement equation (29) yields

$$\ddot{Q}_j(t) + \theta_j^2 Q_j(t) = P_n \cos\omega t\Big\{\theta_{JC} + \cos\frac{a_k}{L}(x_0 + ct + \frac{1}{2}at^2) - A_k \sin\frac{a_k}{L}(x_0 + ct + \frac{1}{2}at^2)$$
$$- B_k \cosh\frac{a_k}{L}(x_0 + ct + \frac{1}{2}at^2) - C_k \sinh\frac{a_k}{L}(x_0 + ct + \frac{1}{2}at^2)\Big\} \tag{30}$$

where

$$P_n = \frac{LMg}{\mu_0 a_k D_0(j,k)} \quad \text{and} \quad \theta_j^2 = \frac{D_1(j,k)}{D_0(j,k)} \tag{31}$$

Using the variation of parameters technique, the solution to equation (30), according to the specified initial conditions (18), is given by

$$Q_j(t) = -\frac{P_n}{2\theta_j}\Bigg(- \Big(\theta_{JC} + A_0 + A_k B_0 + B_k A_0' + C_k B_0'\Big)\Big(\frac{1}{\Omega_1} + \frac{1}{\Omega_2}\Big)$$

$$+ 2\Big(A_2 - A_k B_2 - B_k A_2 - C_k B_2'\Big)\Big(\frac{1}{\Omega_1^3} + \frac{1}{\Omega_2^3}\Big)$$

$$- 24\Big(A_4 - A_k B_4 - B_k A_4 - C_k B_4\Big)\Big(\frac{1}{\Omega_1^5} + \frac{1}{\Omega_2^5}\Big) + 720 B_6\Big(A_k + C_k\Big)\Big(\frac{1}{\Omega_1^7} + \frac{1}{\Omega_2^7}\Big)\Big) \cos\theta_j t$$

$$+ \Big(\Big(A_1 + A_k B_1 + B_k A_1' + C_k B_1'\Big)\Big(\frac{1}{\Omega_1^2} + \frac{1}{\Omega_2^2}\Big)$$

$$- 6\Big(A_3 - A_k B_3 - B_k A_3 - C_k B_3\Big)\Big(\frac{1}{\Omega_1^4} + \frac{1}{\Omega_2^34}\Big) - 120\Big(A_k + C_k\Big)\Big(\frac{1}{\Omega_1^6} + \frac{1}{\Omega_2^6}\Big)\Big) \sin\theta_j t$$

$$- \Big(\Big(\theta JC + A_0 + A_1 t + A_2 t^2 + A_3 t^3 + A_4 t^4\Big)\Big(\frac{\cos\Omega_1 t}{\Omega_1} + \frac{\cos\Omega_2 t}{\Omega_2}\Big)$$

$$+ \Big(A_1 + 2A_2 t + 3A_3 t^2 + 4A_4 t^3\Big)\Big(\frac{\sin\Omega_1 t}{\Omega_1^2} + \frac{\sin\Omega_2 t}{\Omega_2^2}\Big) + \Big(2A_2 + 6A_3 t + 12 A_4 t^2\Big)\Big(\frac{\cos\Omega_1 t}{\Omega_1^3} + \frac{\cos\Omega_2 t}{\Omega_2^3}\Big)$$

$$- \Big(6A_3 + 24A_4 t\Big)\Big(\frac{\sin\Omega_1 t}{\Omega_1^4} + \frac{\sin\Omega_2 t}{\Omega_2^4}\Big) - 24A_4\Big(\frac{\cos\Omega_1}{\Omega_1^5} + \frac{\cos\Omega_2 t}{\Omega_2^5}\Big)\Big)$$

$$- A_k\Big(- \Big(B_0 + B_1 t + B_2 t^2 + B_3 t^3 + B_4 t^4 + B_5 t^5 + B_6 t^6\Big)\Big(\frac{\cos\Omega_1 t}{\Omega_1} + \frac{\cos\Omega_2 t}{\Omega_2}\Big)$$

$$+ \Big(B_1 + 2B_2 t + 3B_3 t^2 + 4B_4 t^3 + 5B_5 t^4 + 6B_6 t^5\Big)\Big(\frac{\sin\Omega_1 t}{\Omega_1^2} + \frac{\sin\Omega_2 t}{\Omega_2^2}\Big)$$

$$+ \Big(2B_2 + 6B_3 t + 12B_4 t^2 + 20B_5 t^3 + 30B_6 t^4\Big)\Big(\frac{\cos\Omega_1 t}{\Omega_1^3} + \frac{\cos\Omega_2 t}{\Omega_2^3}\Big)$$

$$- \Big(6B_3 + 24B_4 t + 60B_5 t^2 + 120B_6 t^3\Big)\Big(\frac{\sin\Omega_1 t}{\Omega_1^4} + \frac{\sin\Omega_2 t}{\Omega_2^4}\Big)$$

$$- \Big(24B_4 + 120B_5 t + 360B_6 t\Big)\Big(\frac{\cos\Omega_1 t}{\Omega_1^5} + \frac{\cos\Omega_2 t}{\Omega_2^5}\Big)\Big)$$

$$+ \Big(120B_5 + 720B_6 t\Big)\Big(\frac{\sin\Omega_1 t}{\Omega_1^6} + \frac{\sin\Omega_2 t}{\Omega_2^6}\Big) + 720B_6\Big(\frac{\cos\Omega_1 t}{\Omega_1^7} + \frac{\cos\Omega_2 t}{\Omega_2^7}\Big)\Big)$$

$$- B_k\Big(- \Big(A_0' + A_1 t + A_2 t^2 + A_3 t^3 + A_4 t^4\Big)\Big(\frac{\cos\Omega_1 t}{\Omega_1} + \frac{\cos\Omega_2 t}{\Omega_2}\Big)$$

$$+ \Big(A_1 + 2A_2 t + 3A_3 t^2 + 4A_4 t^3\Big)\Big(\frac{\sin\Omega_1 t}{\Omega_1^2} + \frac{\sin\Omega_2 t}{\Omega_2^2}\Big) + \Big(2A_2 + 6A_3 t + 12A_4 t^2\Big)\Big(\frac{\cos\Omega_1 t}{\Omega_1^3} + \frac{\cos\Omega_2 t}{\Omega_2^3}\Big)$$

$$- \Big(6A_3 + 24A_4 t\Big)\Big(\frac{\sin\Omega_1 t}{\Omega_1^4} + \frac{\sin\Omega_2 t}{\Omega_2^4}\Big) - 24A_4\Big(\frac{\cos\Omega_1 t}{\Omega_1^5} + \frac{\cos\Omega_2 t}{\Omega_2^5}\Big)\Big)$$

$$- C_k\Big(- \Big(B_0' + B_1 t + B_2' t^2 + B_3 t^3 + B_4 t^4 + B_5 t^5 + B_6 t^6\Big)\Big(\frac{\cos\Omega_1}{\Omega_1} + \frac{\cos\Omega_2 t}{\Omega_2}\Big)$$

$$+ \Big(B_1' + 2B_2' t + 3B_3 t^2 + 4B_4 t^3 + 5B_5 t^4 + 6B_6 t^5\Big)\Big(\frac{\sin\Omega_1 t}{\Omega_1^2} + \frac{\sin\Omega_2 t}{\Omega_2^2}\Big)$$

$$+ \Big(2B_2' + 6B_3 t + 12B_4 t^2 + 20B_5 t^3 + 30B_6 t^4\Big)\Big(\frac{\cos\Omega_1 t}{\Omega_1^3} + \frac{\cos\Omega_2 t}{\Omega_2^3}\Big)$$

$$- \Big(6B_3 + 24B_4 t + 60B_5 t^2 + 120B_6 t^3\Big)\Big(\frac{\sin\Omega_1 t}{\Omega_1^4} + \frac{\sin\Omega_2 t}{\Omega_2^4}\Big)$$

$$- \Big(24B_4 + 120B_5 t + 360B_6 t\Big)\Big(\frac{\cos\Omega_1 t}{\Omega_1^5} + \frac{\cos\Omega_2}{\Omega_2^5}\Big)\Big)$$

$$+ \Big(120B_5 + 720B_6 t\Big)\Big(\frac{\sin\Omega_1 t}{\Omega_1^6} + \frac{\sin\Omega_2 t}{\Omega_2^6}\Big) + 720B_6\Big(\frac{\cos\Omega_1 t}{\Omega_1^7} + \frac{\cos\Omega_2 t}{\Omega_2^7}\Big)\Big) \cos\theta_j t +$$

$$\Big(\Big(\theta JC + A_0 + A_1 t + A_2 t^2 + A_3 t^3 + A_4 t^4\Big)\Big(\frac{\sin\Omega_1}{\Omega_1} + \frac{\sin\Omega_2 t}{\Omega_2}\Big)$$

$$
\begin{aligned}
&+\left(A_1+2A_2t+3A_3t^2+4A_4t^3\right)\left(\frac{\cos\Omega_1 t}{\Omega_1^2}+\frac{\cos\Omega_2 t}{\Omega_2^2}\right)-\left(2A_2+6A_3t+12A_4t^2\right)\left(\frac{\sin\Omega_1 t}{\Omega_1^3}+\frac{\sin\Omega_2 t}{\Omega_2^3}\right)\\
&-\left(6A_3+24A_4t\right)\left(\frac{\cos\Omega_1 t}{\Omega_1^4}+\frac{\cos\Omega_2 t}{\Omega_2^4}\right)+24A_4\left(\frac{\sin\Omega_1 t}{\Omega_1^5}+\frac{\sin\Omega_2 t}{\Omega_2^5}\right)\Bigg)\\
&-A_k\Bigg(\left(B_0+B_1t+B_2t^2+B_3t^3+B_4t^4+B_5t^5+B_6t^6\right)\left(\frac{\sin\Omega_1 t}{\Omega_1}+\frac{\sin\Omega_2 t}{\Omega_2}\right)\\
&+\left(B_1+2B_2t+3B_3t^2+4B_4t^3+5B_5t^4+6B_6t^5\right)\left(\frac{\cos\Omega_1 t}{\Omega_1^2}+\frac{\cos\Omega_2 t}{\Omega_2^2}\right)\\
&-\left(2B_2+6B_3t+12B_4t^2+20B_5t^3+30B_6t^4\right)\left(\frac{\sin\Omega_1 t}{\Omega_1^3}+\frac{\sin\Omega_2 t}{\Omega_2^3}\right)\\
&-\left(6B_3+24B_4t+60B_5t^2+120B_6t^3\right)\left(\frac{\cos\Omega_1 t}{\Omega_1^4}+\frac{\cos\Omega_2 t}{\Omega_2^4}\right)\\
&+\left(24B_4+120B_5t+360B_6t\right)\left(\frac{\sin\Omega_1 t}{\Omega_1^5}+\frac{\sin\Omega_2 t}{\Omega_2^5}\right)\Bigg)\\
&+\left(120B_5+720B_6t\right)\left(\frac{\cos\Omega_1 t}{\Omega_1^6}+\frac{\cos\Omega_2 t}{\Omega_2^6}\right)-720B_6\left(\frac{\sin\Omega_1 t}{\Omega_1^7}+\frac{\sin\Omega_2 t}{\Omega_2^7}\right)\Bigg)\\
&-B_k\Bigg(\left(A_0'+A_1t+A_2t^2+A_3t^3+A_4t^4\right)\left(\frac{\sin\Omega_1 t}{\Omega_1}+\frac{\sin\Omega_2 t}{\Omega_2}\right)\\
&+\left(A_1+2A_2t+3A_3t^2+4A_4t^3\right)\left(\frac{\cos\Omega_1 t}{\Omega_1^2}+\frac{\cos\Omega_2 t}{\Omega_2^2}\right)-\left(2A_2+6A_3t+12A_4t^2\right)\left(\frac{\sin\Omega_1 t}{\Omega_1^3}+\frac{\sin\Omega_2 t}{\Omega_2^3}\right)\\
&-\left(6A_3+24A_4t\right)\left(\frac{\cos\Omega_1 t}{\Omega_1^4}+\frac{\cos\Omega_2 t}{\Omega_2^4}\right)+24A_4\left(\frac{\sin\Omega_1 t}{\Omega_1^5}+\frac{\sin\Omega_2 t}{\Omega_2^5}\right)\Bigg)\\
&-C_k\Bigg(\left(B_0'+B_1't+B_2't^2+B_3t^3+B_4t^4+B_5t^5+B_6t^6\right)\left(\frac{\sin\Omega_1 t}{\Omega_1}+\frac{\sin\Omega_2 t}{\Omega_2}\right)\\
&+\left(B_1'+2B_2't+3B_3t^2+4B_4t^3+5B_5t^4+6B_6t^5\right)\left(\frac{\cos\Omega_1 t}{\Omega_1^2}+\frac{\cos\Omega_2 t}{\Omega_2^2}\right)\\
&-\left(2B_2'+6B_3t+12B_4t^2+20B_5t^3+30B_6t^4\right)\left(\frac{\sin\Omega_1 t}{\Omega_1^3}+\frac{\sin\Omega_2 t}{\Omega_2^3}\right)\\
&-\left(6B_3+24B_4t+60B_5t^2+120B_6t^3\right)\left(\frac{\cos\Omega_1 t}{\Omega_1^4}+\frac{\cos\Omega_2 t}{\Omega_2^4}\right)\\
&+\left(24B_4+120B_5t+360B_6t\right)\left(\frac{\sin\Omega_1 t}{\Omega_1^5}+\frac{\sin\Omega_2 t}{\Omega_2^5}\right)\Bigg)\\
&+\left(120B_5+720B_6t\right)\left(\frac{\cos\Omega_1 t}{\Omega_1^6}+\frac{\cos\Omega_2 t}{\Omega_2^6}\right)-720B_6\left(\frac{\sin\Omega_1 t}{\Omega_1^7}+\frac{\sin\Omega_2 t}{\Omega_2^7}+\right)\Bigg)\Bigg)\sin\theta_j t \qquad (32)
\end{aligned}
$$

where

$$
\begin{aligned}
&A_0=1-k_0x_0^2,\quad A_1=2ck_0x_0,\quad A_2=-k_0(ax_0+c^2),\quad A_3=-ack_0, A_4=\frac{1}{4}a^2k_0\ \text{ and }\ A_0^1=1+k_0x_0^2\\
&B_0=x_0-k_1x_0^3,\quad B_1=c-3cx_0^2,\quad B_2=\frac{1}{2}a-(\frac{3}{2}ax_0+3c^2x_0),\quad B_3=-(3acx_0+c^3),\quad B_4=-(\frac{5}{4}x_0a^2+\frac{3}{2}ac^2)\\
&B_5=-a^2c,\quad B_6=\frac{1}{8}a^3,\quad B_0^1=x_0+k_1x_0^3,\quad B_1^1=c+3cx_0^2\ \text{ and }\ B_2^1=\frac{1}{2}a+(\frac{3}{2}ax_0+3c^2x_0)\\
&\Omega_1=\theta_m+\omega,\quad \Omega_2=\theta_m-\omega_2,\quad k_0=\frac{\gamma^2}{2},\quad k_1=\frac{\gamma^3}{6},\quad \gamma=\frac{a_k}{L} \qquad (33)
\end{aligned}
$$

Substituting equation (33) into equation (19) and simplifying yields.

$$
\begin{aligned}
q_j^*(x,t) = \sum_{j=0}^{\infty} \Bigg\{ &- \frac{P_n}{2\theta_j \Omega_1^7 \Omega_2^7} \Bigg(\Bigg(- \Big(\theta_{JC} + A_0 + A_k B_0 + B_k A_0' + C_k B_0' \Big) \Big(\Omega_1^6 \Omega_2^7 + \Omega_1^7 \Omega_2^6 \Big) \\
&+ 2\Big(A_2 - A_k B_2 - B_k A_2 - C_k B_2' \Big) \Big(\Omega_1^4 \Omega_2^7 + \Omega_1^7 \Omega_2^4 \Big) \\
&- 24\Big(A_4 - A_k B_4 - B_k A_4 - C_k B_4 \Big) \Big(\Omega_1^2 \Omega_2^7 + \Omega_1^7 \Omega_2^2 \Big) + 720 B_6 \Big(A_k + C_k \Big) \Big(\Omega_2^7 + \Omega_1^7 \Big) \Bigg) \cos\theta_j t \\
&+ \Bigg(\Big(A_1 + A_k B_1 + B_k A_1' + C_k B_1' \Big) \Big(\Omega_1^5 \Omega_2^7 + \Omega_1^7 \Omega_2^5 \Big) \\
&- 6\Big(A_3 - A_k B_3 - B_k A_3 - C_k B_3 \Big) \Big(\Omega_1^3 \Omega_2^7 + \Omega_1^7 \Omega_2^3 \Big) - 120\Big(A_k + C_k \Big) \Big(\Omega_1 \Omega_2^7 + \Omega_1^7 \Omega_2 \Big) \Bigg) \sin\theta_j t \\
&\Bigg(- \Big(\theta JC + A_0 + A_1 t + A_2 t^2 + A_3 t^3 + A_4 t^4 \Big) \Big(\Omega_1^6 \Omega_2^7 \cos\Omega_1 t + \Omega_1^7 \Omega_2^6 \cos\Omega_2 t \Big) \\
&+ \Big(A_1 + 2A_2 t + 3A_3 t^2 + 4A_4 t^3 \Big) \Big(\Omega_1^5 \Omega_2^7 \sin\Omega_1 t + \Omega_1^7 \Omega_2^5 \sin\Omega_2 t \Big) \\
&+ \Big(2A_2 + 6A_3 t + 12 A_4 t^2 \Big) \Big(\Omega_1^4 \Omega_2^7 \cos\Omega_1 t + \Omega_1^4 \Omega_2^7 \cos\Omega_2 t \Big) - \Big(6A_3 + 24 A_4 t \Big) \Big(\Omega_1^3 \Omega_2^7 \sin\Omega_1 t + \Omega_1^7 \Omega_2^3 \sin\Omega_2 t \Big) \\
&- 24 A_4 \Big(\Omega_1^2 \Omega_2^7 \cos\Omega_1 t + \Omega_1^7 \Omega_2^2 \cos\Omega_2 t \Big) \Big) - A_k \Big(- \Big(B_0 + B_1 t + B_2 t^2 + B_3 t^3 + B_4 t^4 + B_5 t^5 \\
&+ B_6 t^6 \Big) \Big(\Omega_1^6 \Omega_2^7 \cos\Omega_1 t + \Omega_1^7 \Omega_2^6 \cos\Omega_2 t \Big) + \Big(B_1 + 2B_2 t + 3B_3 t^2 + 4B_4 t^3 + 5B_5 t^4 + 6B_6 t^5 \Big) \Big(\Omega_1^5 \Omega_2^7 \sin\Omega_1 t \\
&+ \Omega_1^7 \Omega_2^5 \sin\Omega_2 t \Big) + \Big(2B_2 + 6B_3 t + 12 B_4 t^2 + 20 B_5 t^3 + 30 B_6 t^4 \Big) \Big(\Omega_1^4 \Omega_2^7 \cos\Omega_1 t + \Omega_1^7 \Omega_2^4 \cos\Omega_2 t \Big) \\
&- \Big(6B_3 + 24 B_4 t + 60 B_5 t^2 + 120 B_6 t^3 \Big) \Big(\Omega_1^3 \Omega_2^7 \sin\Omega_1 t + \Omega_1^7 \Omega_2^3 \sin\Omega_2 t \Big) \\
&- \Big(24 B_4 + 120 B_5 t + 360 B_6 t \Big) \Big(\Omega_1^2 \Omega_2^7 \cos\Omega_1 t + \Omega_1^7 \Omega_2^2 \cos\Omega_2 t \Big) \Big) \\
&+ \Big(120 B_5 + 720 B_6 t \Big) \Big(\Omega_1 \Omega_2^7 \sin\Omega_1 t + \Omega_1^7 \Omega_2 \sin\Omega_2 t \Big) + 720 B_6 \Big(\Omega_2^7 \cos\Omega_1 t + \Omega_1^7 \cos\Omega_2 t \Big) \Big) \\
&- B_k \Big(\Big(A_0' + A_1 t + A_2 t^2 + A_3 t^3 + A_4 t^4 \Big) \Big(\Omega_1^6 \Omega_2^7 \cos\Omega_1 t + \Omega_1^7 \Omega_2^6 \cos\Omega_2 t \Big) \\
&+ \Big(A_1 + 2A_2 t + 3A_3 t^2 + 4A_4 t^3 \Big) \Big(\Omega_1^5 \Omega_2^7 \sin\Omega_1 t + \Omega_1^7 \Omega_2^5 \sin\Omega_2 t \Big) + \Big(2A_2 + 6A_3 t + 12 A_4 t^2 \Big) \Big(\Omega_1^4 \Omega_2^7 \cos\Omega_1 t \\
&+ \Omega_1^4 \Omega_2^7 \cos\Omega_2 t \Big) - \Big(6A_3 + 24 A_4 t \Big) \Big(\Omega_1^3 \Omega_2^7 \sin\Omega_1 t + \Omega_1^7 \Omega_2^3 \sin\Omega_2 t \Big) - 24 A_4 \Big(\Omega_1^2 \Omega_2^7 \cos\Omega_1 t + \Omega_1^7 \Omega_2^2 \cos\Omega_2 t \Big) \Big) \\
&- C_k \Big(- \Big(B_0' + B_1 t + B_2' t^2 + B_3 t^3 + B_4 t^4 + B_5 t^5 + B_6 t^6 \Big) \Big(\Omega_1^6 \Omega_2^7 \cos\Omega_1 t + \Omega_1^7 \Omega_2^6 \cos\Omega_2 t \Big) \\
&+ \Big(B_1' + 2B_2' t + 3B_3 t^2 + 4B_4 t^3 + 5B_5 t^4 + 6B_6 t^5 \Big) \Big(\Omega_1^5 \Omega_2^7 \sin\Omega_1 t + \Omega_1^7 \Omega_2^5 \sin\Omega_2 t \Big) \\
&+ \Big(2B_2' + 6B_3 t + 12 B_4 t^2 + 20 B_5 t^3 + 30 B_6 t^4 \Big) \Big(\Omega_1^4 \Omega_2^7 \cos\Omega_1 t + \Omega_1^7 \Omega_2^4 \cos\Omega_2 t \Big) \\
&- \Big(6B_3 + 24 B_4 t + 60 B_5 t^2 + 120 B_6 t^3 \Big) \Big(\Omega_1^3 \Omega_2^7 \sin\Omega_1 t + \Omega_1^7 \Omega_2^3 \sin\Omega_2 t \Big) \\
&- \Big(24 B_4 + 120 B_5 t + 360 B_6 t \Big) \Big(\Omega_1^2 \Omega_2^7 \cos\Omega_1 t + \Omega_1^7 \Omega_2^2 \cos\Omega_2 t \Big) \Big) \\
&+ \Big(120 B_5 + 720 B_6 t \Big) \Big(\Omega_1 \Omega_2^7 \sin\Omega_1 t + \Omega_1^7 \Omega_2 \sin\Omega_2 t \Big) + 720 B_6 \Big(\Omega_2^7 \cos\Omega_1 t + \Omega_1^7 \cos\Omega_2 t \Big) \Big) \cos\theta_j t
\end{aligned}
$$

$$
\begin{aligned}
&+\Bigg(\bigg(\theta_{JC}+A_0+A_1t+A_2t^2+A_3t^3+A_4t^4\bigg)\bigg(\Omega_1^6\Omega_2^7\sin\Omega_1t+\Omega_1^7\Omega_2^6\sin\Omega_2t\bigg)+\\
&+\bigg(A_1+2A_2t+3A_3t^2+4A_4t^3\bigg)\bigg(\Omega_1^5\Omega_2^7\cos\Omega_1t+\Omega_1^7\Omega_2^5\cos\Omega_2t\bigg)-\bigg(2A_2+6A_3t+12A_4t^2\bigg)\bigg(\Omega_1^4\Omega_2^7\sin\Omega_1t\\
&+\Omega_1^7\Omega_2^4\sin\Omega_2t\bigg)-\bigg(6A_3+24A_4t\bigg)\bigg(\Omega_1^3\Omega_2^7\cos\Omega_1t+\Omega_1^7\Omega_2^3\cos\Omega_2t\bigg)+24A_4\bigg(\Omega_1^2\Omega_2^7\sin\Omega_1t+\Omega_1^7\Omega_2^2\sin\Omega_2t\bigg)\Bigg)\\
&-A_k\Bigg(\bigg(B_0+B_1t+B_2t^2+B_3t^3+B_4t^4+B_5t^5+B_6t^6\bigg)\bigg(\Omega_1^6\Omega_2^7\sin\Omega_1t+\Omega_1^7\Omega_2^6\sin\Omega_t2\bigg)\\
&+\bigg(B_1+2B_2t+3B_3t^2+4B_4t^3+5B_5t^4+6B_6t^5\bigg)\bigg(\Omega_1^5\Omega_2^7\cos\Omega_1t+\Omega_1^7\Omega_2^5\cos\Omega_2t\bigg)\\
&-\bigg(2B_2+6B_3t+12B_4t^2+20B_5t^3+30B_6t^4\bigg)\bigg(\Omega_1^4\Omega_2^7\sin\Omega_1t+\Omega_1^7\Omega_2^4\sin\Omega_2t\bigg)\\
&-\bigg(6B_3+24B_4t+60B_5t^2+120B_6t^3\bigg)\bigg(\Omega_1^3\Omega_2^7\cos\Omega_1t+\Omega_1^7\Omega_2^3\cos\Omega_2t\bigg)\\
&+\bigg(24B_4+120B_5t+360B_6t\bigg)\bigg(\Omega_1^2\Omega_2^7\sin\Omega_1t+\Omega_1^7\Omega_2^2\sin\Omega_2t\bigg)\bigg)\\
&+\bigg(120B_5+720B_6t\bigg)\bigg(\Omega_1\Omega_2^7\cos\Omega_1t+\Omega_1^7\Omega_2\cos\Omega_2t\bigg)-720B_6\bigg(\Omega_2^7\sin\Omega_1t+\Omega_1^7\sin\Omega_2t\bigg)\Bigg)\\
&-B_k\Bigg(\bigg(A_0'+A_1t+A_2t^2+A_3t^3+A_4t^4\bigg)\bigg(\Omega_1^6\Omega_2^7\sin\Omega_1t+\Omega_1^7\Omega_2^6\sin\Omega_2t\bigg)+\\
&+\bigg(A_1+2A_2t+3A_3t^2+4A_4t^3\bigg)\bigg(\Omega_1^5\Omega_2^7\cos\Omega_1t+\Omega_1^7\Omega_2^5\cos\Omega_2t\bigg)-\bigg(2A_2+6A_3t+12A_4t^2\bigg)\bigg(\Omega_1^4\Omega_2^7\sin\Omega_1t\\
&+\Omega_1^7\Omega_2^4\sin\Omega_2t\bigg)-\bigg(6A_3+24A_4t\bigg)\bigg(\Omega_1^3\Omega_2^7\cos\Omega_1t+\Omega_1^7\Omega_2^3\cos\Omega_2t\bigg)+24A_4\bigg(\Omega_1^2\Omega_2^7\sin\Omega_1t+\Omega_1^7\Omega_2^2\sin\Omega_2t\bigg)\Bigg)\\
&-C_k\Bigg(\bigg(B_0'+B_1't+B_2't^2+B_3t^3+B_4t^4+B_5t^5+B_6t^6\bigg)\bigg(\Omega_1^6\Omega_2^7\sin\Omega_1t+\Omega_1^7\Omega_2^6\sin\Omega_t2\bigg)\\
&+\bigg(B_1'+2B_2't+3B_3t^2+4B_4t^3+5B_5t^4+6B_6t^5\bigg)\bigg(\Omega_1^5\Omega_2^7\cos\Omega_1t+\Omega_1^7\Omega_2^5\cos\Omega_2t\bigg)\\
&-\bigg(2B_2'+6B_3t+12B_4t^2+20B_5t^3+30B_6t^4\bigg)\bigg(\Omega_1^4\Omega_2^7\sin\Omega_1t+\Omega_1^7\Omega_2^4\sin\Omega_2t\bigg)\\
&-\bigg(6B_3+24B_4t+60B_5t^2+120B_6t^3\bigg)\bigg(\Omega_1^3\Omega_2^7\cos\Omega_1t+\Omega_1^7\Omega_2^3\cos\Omega_2t\bigg)\\
&+\bigg(24B_4+120B_5t+360B_6t\bigg)\bigg(\Omega_1^2\Omega_2^7\sin\Omega_1t+\Omega_1^7\Omega_2^2\sin\Omega_2t\bigg)\bigg)\\
&+\bigg(120B_5+720B_6t\bigg)\bigg(\Omega_1\Omega_2^7\cos\Omega_1t+\Omega_1^7\Omega_2\cos\Omega_2t\bigg)-720B_6\bigg(\Omega_2^7\sin\Omega_1t\\
&+\Omega_1^7\sin\Omega_2t\bigg)\bigg)\sin\theta_jt\bigg)\Bigg\}\times\bigg(\sin\frac{a_jx}{L}+A_j\cos\frac{a_jx}{L}+B_j\sinh\frac{a_jx}{L}+C_j\cosh\frac{a_jx}{L}\bigg)\Bigg\} \qquad (34)
\end{aligned}
$$

Equation (34) provides the transverse displacement solution for a non-uniform Rayleigh beam under the influence of a moving distributed force with arbitrary boundary conditions.

4.2 Non-uniform Rayleigh Beam Traversed by Moving Mass

If the inertia term is retained, then it is termed the moving mass problem. In this case, the solution to the entire equation (27) is required. That is, if $\epsilon_0 \neq 0$, we have

$$D_0(j,k)\ddot{Q}_j(t) + D_1(j,k)Q_j(t) + \epsilon_0 \cos\omega t\Big\{\triangle_1(n,j,k)\ddot{Q}_j(t) + 2L(c+at)\triangle_2(n,j,k)\dot{Q}_j(t)$$
$$+ \Big(L(c+at)\triangle_3(n,j,k) + aL\triangle_2(n,j,k)\Big)Q_j(t)\Big\} = \frac{LMg\cos\omega t}{\mu_0 a_k}\Big\{\theta_{JC} + \cos\frac{a_k}{L}p^*(t) - A_k + \sin\frac{a_k}{L}p^*(t)$$
$$- B_k + \cosh\frac{a_k}{L}p^*(t) - C_k + \sinh\frac{a_k}{L}p^*(t)\Big\} \tag{35}$$

where

$$\triangle_1(n,m,k) = \frac{1}{4}B_1(j,k) + \frac{1}{\pi}\sum_0^\infty \frac{\cos(2n+1)\pi p^*(t)}{(2n+1)}B_{1A}(n,j,k) - \frac{1}{\pi}\sum_0^\infty \frac{\sin(2n+1)\pi p^*(t)}{(2n+1)}B_{1B}(n,j,k)$$

$$\triangle_2(n,j,k) = \frac{1}{4}B_2(j,k) + \frac{1}{\pi}\sum_0^\infty \frac{\cos(2n+1)\pi p^*(t)}{(2n+1)}B_{2A}(n,j,k) - \frac{1}{\pi}\sum_0^\infty \frac{\sin(2n+1)\pi p^*(t)}{(2n+1)}B_{2B}(n,j,k)$$

$$\triangle_3(n,j,k) = \frac{1}{4}B_3(j,k) + \frac{1}{\pi}\sum_0^\infty \frac{\cos(2n+1)\pi p^*(t)}{(2n+1)}B_{3A}(n,j,k) - \frac{1}{\pi}\sum_0^\infty \frac{\sin(2n+1)\pi p^*(t)}{(2n+1)}B_{3B}(n,j,k) \tag{36}$$

Further simplification and rearrangement of equation (35) lead to

$$\ddot{Q}_j(t) + DC_1\dot{Q}_j(t) + DC_2Q_j(t) = DC_3 \tag{37}$$

where

$$DC_1 = \frac{2L(c+at)\epsilon_0\cos\omega t\triangle_2(n,j,k)}{D_0(j,k) + \epsilon_0\cos\omega t\triangle_1(n,j,k)}$$
$$DC_2 = \frac{D_1(j,k)L\epsilon_0(C+at)^2\cos\omega t\triangle_3(n,j,k) + aL\epsilon_0\cos\omega t\triangle_2(n,j,k)}{D_0(j,k) + \epsilon_0\cos\omega t\triangle_1(n,j,k)}$$
$$DC_3 = \frac{LMg\cos\omega t}{(D_0(m,k) + \Gamma_0\cos\omega t\triangle_1(n,j,k))\mu_0 a_k}\Big(\theta_{JC} + \cos\frac{a_k}{L}p^*(t) - A_k + \sin\frac{a_k}{L}p^*(t) - B_k + \cosh\frac{a_k}{L}p^*(t)$$
$$- C_k + \sinh\frac{a_k}{L}p^*(t)\Big) \tag{38}$$

The fourth order Runge-Kutta scheme is used to solve (37) to obtain transverse displacement solution for a non-uniform Rayleigh beam under the influence of a moving distributed mass with arbitrary boundary conditions.

5 Illustrative Examples

This section presents illustrative examples of classical boundary conditions, demonstrating the application of the analytical framework developed in this paper

5.1 Clamped-clamped Boundary Condition

For a beam with clamped-clamped ends, deflection and slope are zero at the boundaries. Specifically, at $x = 0$ and $x = L$, the boundary conditions are

$$q^*(0,t) = q^*(L,t) = 0, \quad \frac{\partial}{\partial x}q^*(0,t) = \frac{\partial}{\partial x}q^*(L,t) = 0 \tag{39}$$

and, hence for the normal modes;

$$Z_j(0,t) = Z_j(L,t) = 0, \quad \frac{\partial}{\partial x}Z_j(0,t) = \frac{\partial}{\partial x}Z_j(L,t) = 0 \tag{40}$$

This implies that;

$$Z_k(0,t) = Z_k(L,t) = 0, \quad \frac{\partial}{\partial x}Z_k(0,t) = \frac{\partial}{\partial x}Z_k(L,t) = 0 \tag{41}$$

Applying equation (40) to equation (25) yields

$$\begin{aligned} &\Rightarrow A_j = \frac{\sinh a_j - \sin a_j}{\cos a_j - A_j \cosh a_j} = \frac{\cos a_j - A_j \cosh a_j}{\sin a_j + \sinh a_j} = -C_j \\ &B_j = -1 \end{aligned} \tag{42}$$

The frequency equation become

$$\Rightarrow \quad \cos a_j \cosh a_j = 1 \tag{43}$$

The expressions for A_k, B_k and C_k can be readily obtained by replacing j with k in equations (42) and (43). Subsequently, substituting these results into equations (34) and (37) yields the displacement responses of a clamped-clamped non-uniform Rayleigh beam to moving distributed forces and masses, respectively.

5.2 One End Clamped and One End Free Condition (Cantilever Beam)

In this illustrative example, we have free right-hand end, and clamped at the left hand end to be consider. According, the boundary condition are:

$$q^*(0,t) = \frac{\partial}{\partial x}q^*(0,t) = 0 \;\; and \;\; \frac{\partial^2}{\partial x^2}q^*(L,t) = \frac{\partial^3}{\partial x^3}q^*(L,t) = 0 \tag{44}$$

Therefore, we have; hand end to be consider. According, the boundary condition are:

$$Z_j(0) = \frac{\partial}{\partial x}Z_j(0) = 0 \;\; and \;\; \frac{\partial^2}{\partial x^2}Z_j(L) = \frac{\partial^3}{\partial x^3}Z_j(L) = 0 \tag{45}$$

This implies that,

$$Z_k(0) = \frac{\partial}{\partial x}Z_k(0) = 0 \;\; and \;\; \frac{\partial^2}{\partial x^2}Z_k(L) = \frac{\partial^3}{\partial x^3}Z_k(L) = 0 \tag{46}$$

Substituting equation (46) into equation (26) yields

$$\Rightarrow A_k = -\frac{\sin a_k + \sinh a_k}{\cos a_k + \cosh a_k} = \frac{\cosh a_k + \cos a_k}{\sin a_k - \sinh a_k} = -C_k$$

$$C_k = -1 \tag{47}$$

And the frequency equation for both end conditions is

$$\cos a_k \cosh a_k = -1 \tag{48}$$

The expressions for A_j, B_j, and C_j can be readily obtained by replacing k with j in equations (47) and (48). Subsequently, substituting these results into equations (34) and (37) yields the displacement responses of a clamped-free non-uniform Rayleigh beam to moving distributed forces and masses, respectively.

6 Discussion of Closed Form Solutions

For the undamped system, it is desirable to examine the phenomenon of resonance. From equation (34), it is clear that the non-uniform Rayleigh beam under variable-magnitude accelerating force and resting on non-uniform bi-parametric foundation reaches a state of resonance whenever

$$\Omega_1 \Omega_2 = 0 \tag{49}$$

and

$$\Omega_1 = 0 \quad \text{or} \quad \Omega_2 = 0 \tag{50}$$

7 Numerical Results and Discussion

To illustrate the foregoing analysis, a numerical investigation was conducted on a non-uniform Rayleigh beam with a length (L) of 12.192 m, subjected to a load velocity (v) of $8.128 m/s$, and the Young's modulus material (E) of $2.109 \times 10^9 N/m^2$ and mass ratio $\epsilon_0 = 0.5$. A parametric study was performed to examine the influence of rotatory inertia factor R_0 and shear modulus G_0 on the beam's displacement response, with R_0 varying between $20kg/m^2$ to $50kg/m^2$ and G_0 ranging from $10000kg/m^2$ to $50000kg/m^2$.

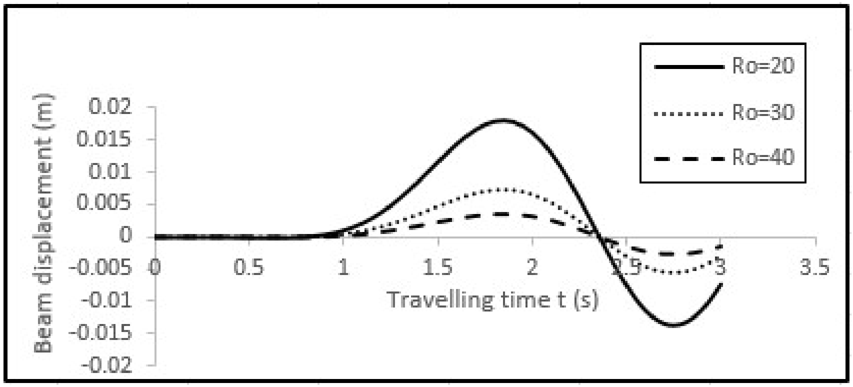

Fig. 1. A clamped-clamped non-uniform Rayleigh beam's displacement response under distributed forces for various values of rotatory inertia R_0 and fixed values of S_0, G_0, and N.

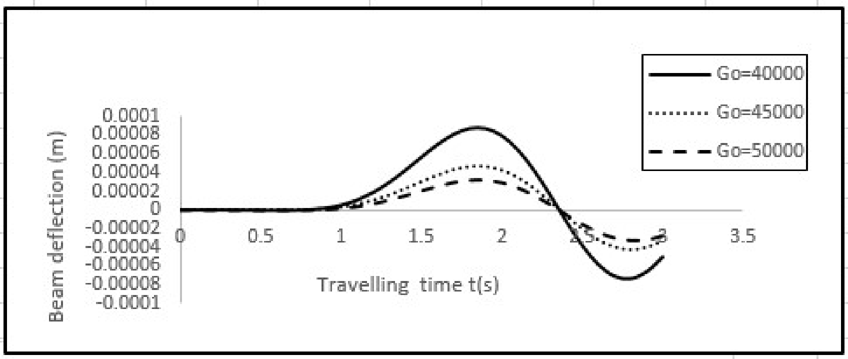

Fig. 2. A clamped-clamped non-uniform Rayleigh beam's displacement response under distributed forces for various values of shear modulus G_0 and fixed values of S_0, R_0, and N.

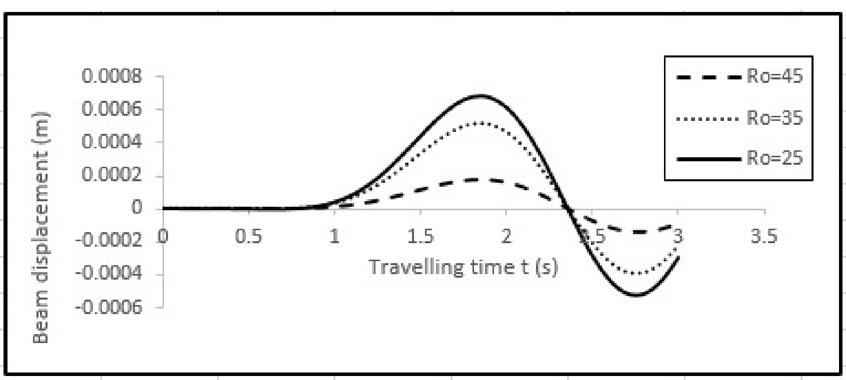

Fig. 3. A clamped-clamped non-uniform Rayleigh beam's displacement response under distributed masses for various values of rotatory inertia R_0 and fixed values of S_0, G_0, and N.

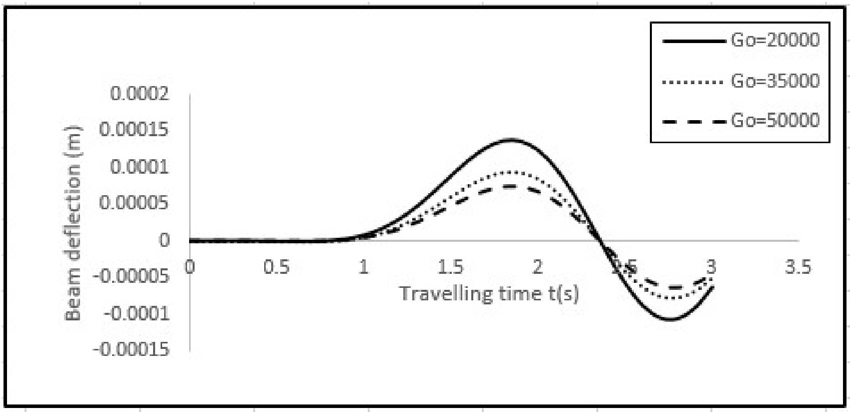

Fig. 4. A clamped-clamped non-uniform Rayleigh beam's displacement response under distributed masses for various values of shear modulus G_0 and fixed values of S_0, R_0, and N.

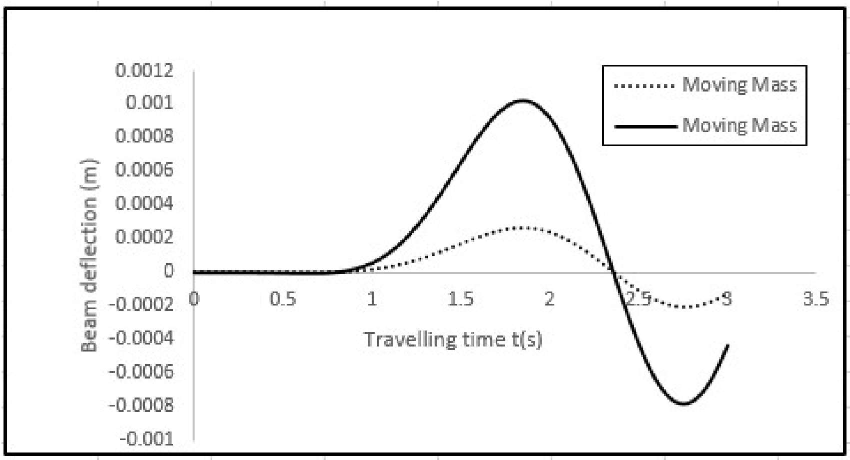

Fig. 5. A comparison between the deflection of moving distributed mass and moving distributed force for non-uniform clamped-clamped Rayleigh beams.

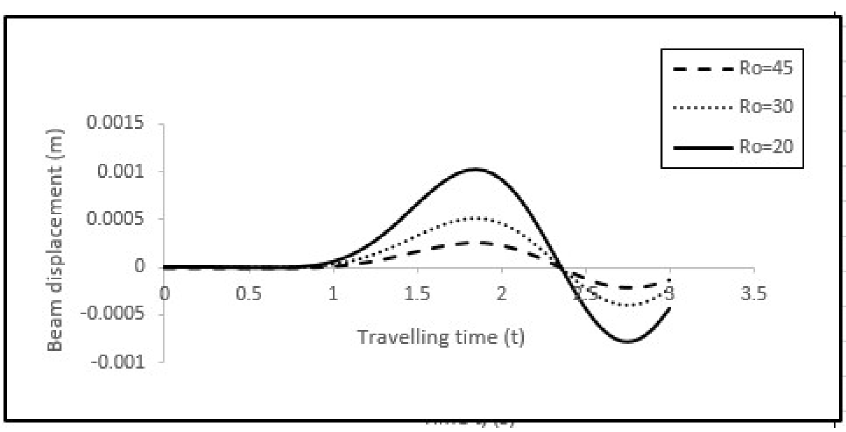

Fig. 6. A clamped-free non-uniform Rayleigh beam's displacement response under distributed forces for various values of rotatory inertia R_0 and fixed values of S_0, G_0, and N.

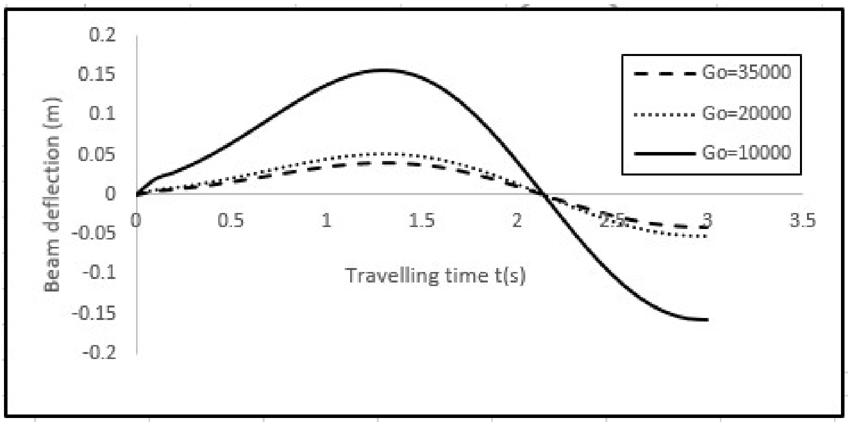

k

Fig. 7. A clamped-free non-uniform Rayleigh beam's displacement response under distributed forces for various values of shear modulus G_0 and fixed values of S_0, R_0, and N.

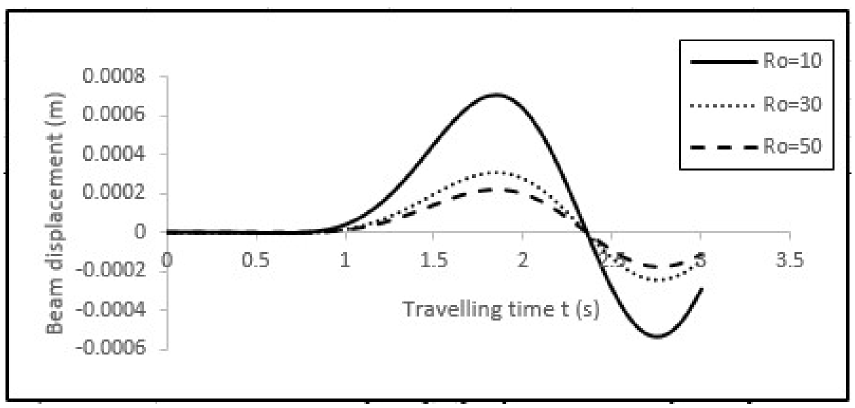

Fig. 8 . A clamped-free non-uniform Rayleigh beam's displacement response under distributed masses for various values of rotatory inertia R_0 and fixed values of S_0, G_0, and N.

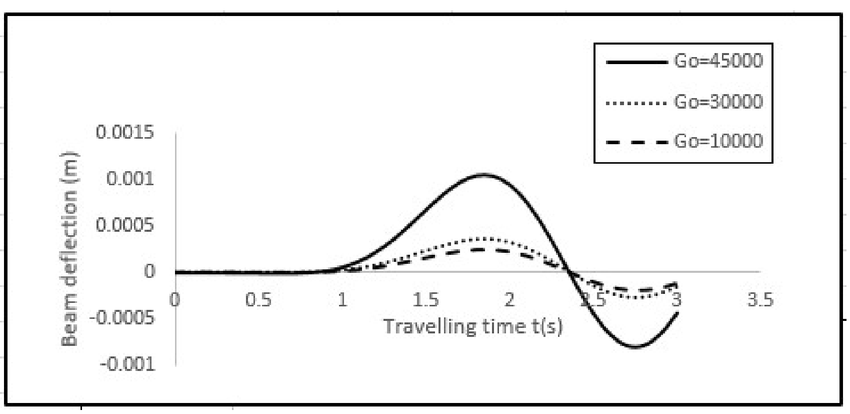

Fig. 9. A clamped-free non-uniform Rayleigh beam's displacement response under distributed masses for various values of shear modulus G_0 and fixed values of S_0, R_0, and N.

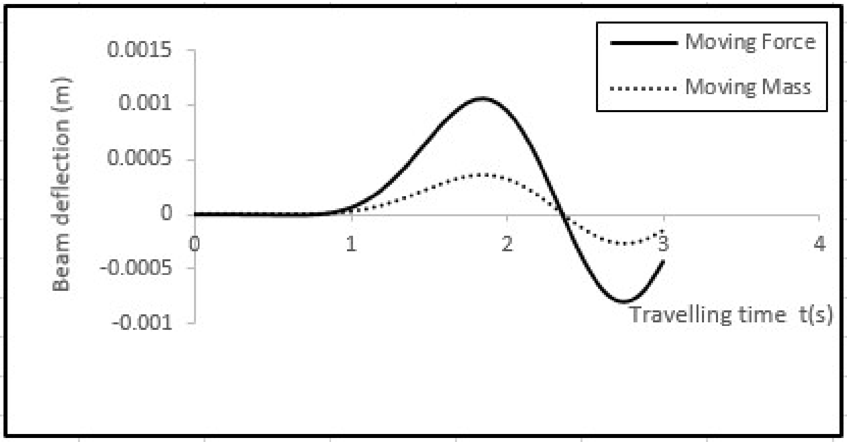

Fig. 10. A comparison between the deflection of moving distributed mass and moving distributed force for non-uniform clamped-free Rayleigh beams.

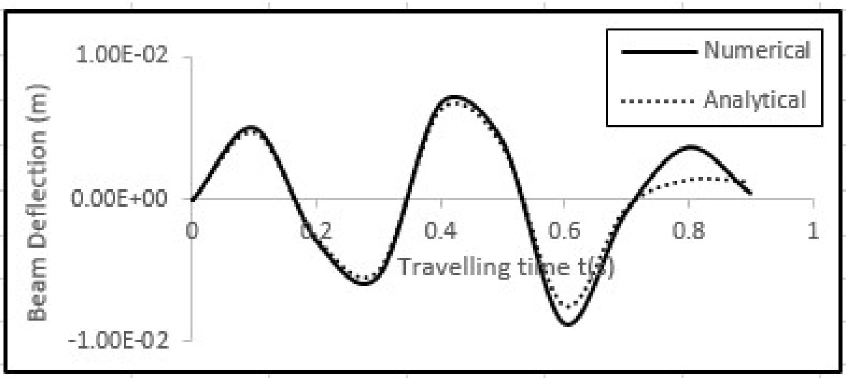

Fig. 11. Comparison of the displacement response of analytical solution and numerical solution of a clamped-clamped non-uniform Rayleigh for fixed values G_0, N, R_0, and S_0.

Seen in Fig 1, the figure shows that the response amplitude of the non-uniform clamped-clamped Rayleigh beam under the action of moving distributed forces diminishes as the values of the rotatory inertia R_0 increase. Similar outcomes are observed in Fig 3, where moving distributed masses traverse the same non-uniform clamped-clamped Rayleigh beam. For a fixed value of Rotatory inertia R_0, foundation stiffness S_0, and axial force N and a various values of shear modulus (G_0), Fig 2 illustrates the clamped-clamped non-uniform Rayleigh beam's response to moving distributed forces. It is found that the beam's deflection decreases as the shear modulus rises. The deflection profile behaves similarly when moving distributed masses traverse a non-uniform clamped-clamped Rayleigh beam, as seen in Fig 4. Fig 5 shows the comparison of transverse displacement responses for non-uniform clamped-clamped Rayleigh beams subjected to moving distributed forces and masses, where foundation stiffness S_0, rotatory inertia R_0, shear modulus G_0 and axial force N are fixed. The results demonstrate that moving distributed forces generate larger response amplitudes than moving distributed masses. Fig 6 presents the deflection profile of a non-uniform clamped-free Rayleigh beam under moving distributed forces for varying rotatory inertia R_0 and fixed values of a foundation stiffness S_0, shear modulus G_0 and axial force N. The results demonstrate that increasing rotatory inertia values reduces beam deflection. This trend is consistently observed in Fig 8, where moving distributed masses traverse the same beam. For a fixed value of rotatory inertia R_0, foundation stiffness S_0, and axial force N and a various values of shear modulus (G_0), Fig 7 illustrates the clamped-free non-uniform Rayleigh beam's response to moving distributed forces. It is found that the beam's deflection decreases as the shear modulus rises. The deflection profile behaves similarly when moving distributed masses traverse a non-uniform clamped-free Rayleigh beam, as seen in Fig 9. Fig 10 shows the comparison of transverse displacement responses for non-uniform clamped-free Rayleigh beams subjected to moving distributed forces and masses, where foundation stiffness S_0, rotatory inertia R_0, shear modulus G_0 and axial force N are fixed. The results demonstrate that moving distributed forces generate larger response amplitudes than moving distributed masses. Figure 11 presents a comparative analysis between numerical and approximate analytical solutions for the deflection response of a clamped-clamped non-uniform Rayleigh beam resting on a bi-parametric foundation, subjected to a moving distributed force and variable-magnitude accelerating mass. The remarkable similarity in amplitude between the two profiles validates the effectiveness of the Runge-Kutta method in addressing this complex dynamic problem. The comparative analysis of closed-form solutions for clamped-clamped and clamped-free boundary conditions reveals that moving distributed forces induce resonance earlier than moving distributed masses. This underscores the vital importance of accounting for both load types in beam design to guarantee structural integrity, vibration control, and ultimately, enhanced safety in bridges, resilience in buildings, and efficiency in industrial machinery.

Additionally, for both clamped-clamped and clamped-free boundary conditions, increasing the values of rotatory inertia and shear modulus leads to a decrease in beam deflection. The observed decrease in beam deflection with increasing rotatory inertia and shear modulus can be attributed to the enhanced stiffness of the beam-foundation system. Specifically, as the rotatory inertia of the beam increases, its resistance to bending and torsion also increases, leading to reduced deflection. Similarly, a higher shear modulus of the foundation indicates a stiffer foundation, providing greater support to the beam and resulting in decreased deflection. Ultimately, the increased stiffness of both the beam and foundation contributes to the reduced deflection of the beam. The reduction in beam deflection due to increased shear modulus of the foundation and rotatory inertia has significant implications for structural design and vibration control. In bridge construction, stiffer foundations and optimized beam design can ensure safer and more durable structures, while in high-rise buildings, reduced deflections mitigate wind-induced vibrations. Similarly, machine foundations, wind turbines, and offshore platforms benefit from improved stability and reduced vibrations. Furthermore, aerospace engineers can enhance aircraft and spacecraft stability through optimized structural design. These findings underscore the importance of considering shear modulus and rotatory inertia in engineering design to minimize deflections, promote structural integrity, and enhance overall system performance.

8 Conclusion

This paper presents a solution approach for the dynamic behaviours of non-uniform Rayleigh beam under variable-magnitude accelerating masses and resting on non-uniform bi-parametric foundation with general boundary Conditions. The approximation procedure based on the generalized Galerkin method. The non-uniform Rayleigh beam's governing fourth-order differential equation with variable and singular coefficients is given closed-form solutions. Considerable attention is paid to the impact of relevant factors such the shear modulus and rotatory inertia factor. Plotted curve analysis reveals that a decrease in the deflection of both clamped-clamped non-uniform Rayleigh beam and non-uniform Rayleigh beam occurs with an increase in structural parameters. Thus, guarantee the safety of accelerating loads of varying magnitude while simultaneously reducing vibration.

References

[1] Ogunlusi T, Awodola T. Dynamic Behaviour of Simply Supported Non-Uniform Rayleigh Beam under Variable-Magnitude Accelerating Masses and Resting on Non-Uniform Bi-parametric Foundation. Asian Research Journal of Mathematics. 2024;20(11).

[2] Omolofe B, Adara EO. Response characteristics of a beam-mass system with general boundary conditions under compressive axial force and accelerating masses. Engineering Reports. 2020;2(2):e12118.

[3] Awodola T, Awe B, Jimoh S. VIBRATION OF NON-UNIFORM BERNOULLI-EULER BEAM UNDER MOVING DISTRIBUTED MASSES RESTING ON PASTERNAK ELASTIC FOUNDATION SUBJECTED TO VARIABLE MAGNITUDE. 2023;.

[4] Jimoh A, Ajoge E. Dynamic analysis of Non-Uniform Rayleigh beam Resting on Bi-Parametric Subgrade under Exponentially Varying Moving Loads. Journal of Applied Mathematics and Bioinformatics. 2019;9(2):1–16.

[5] Omolofe B, Adara EO. Dynamic amplification factor and interactions of a beam under compressive axial force and load travelling at varying velocity. Forces in Mechanics. 2023;13:100241.

[6] Oni S, Ogunyebi S. Dynamical analysis of a prestressed elastic beam with general boundary conditions under the action of uniform distributed masses. Journal of the Nigerian Association of Mathematical Physics. 2008;12.

[7] Oni S, Awodola T. Dynamic response under a moving load of an elastically supported non-prismatic Bernoulli-Euler beam on variable elastic foundation. Latin American Journal of Solids and Structures. 2010;p. 3–20.

[8] Jimoh S. On modal-asymptotic analysis to prestressed thick beam on bi-parametric foundation subjected to moving loads. Achievers Journal of Scientific Research. 2021;3(2):28–46.

[9] Oni S, Ogunbamike O. Dynamic Behaviour Of Non-Prismatic Rayleigh Beam On Pasternak Foundation And Under Partially Distributed Masses Moving At Varying Velocities. Journal of the Nigerian Mathematical Society. 2014;33(1-3):285–310.

[10] Andi EA, Oni ST. Dynamic behaviour under moving distributed masses of nonuniform Rayleigh beam with general boundary conditions. Chinese Journal of Mathematics. 2014;2014(1):565826.

[11] Fryba L. Vibration of solids and structures under moving loads, the netherlands: Noordhoff International. Groningen;.

[12] Timoshenko SP. On the correction for shear of the differential equation for transverse vibrations of prismatic bars. Phil Mag Ser. 1921;41:744–764.

[13] Biot MA. Bending of an infinite beam on an elastic foundation. 1937;.